LA-UR- 96-2645

Title: An Integrating Image Detector for High Energy Neutrons

CONF-960690--10

Author(s): Chris Morris, V. Armijo, L. G. Atencio, A. Bridge, A. Gavron, G. Hart, K. Morley, T. Mottershead, G. J. Yates, and John Zumbro

Submitted to: *5th International Conference on Applications of Nuclear Techniques: Neutrons in Research and Industry*
Crete, Greece
June 9–15, 1996

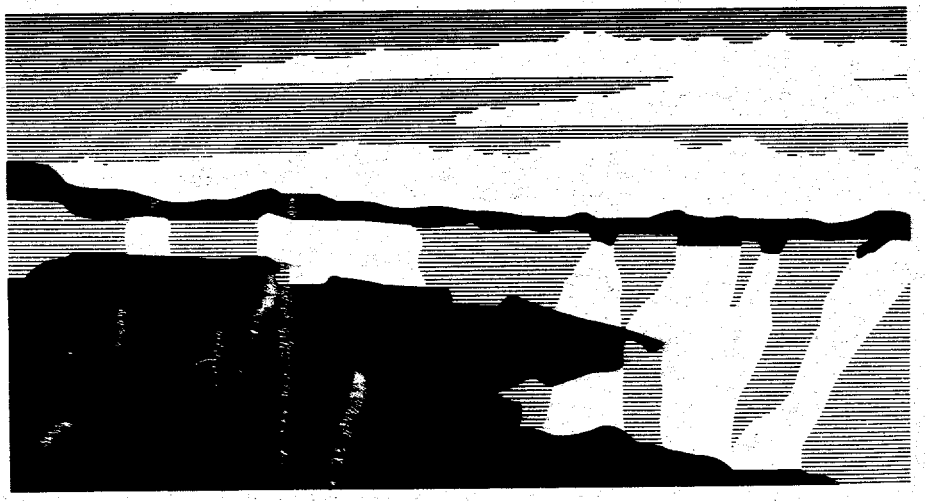

Los Alamos
NATIONAL LABORATORY

Form No. 836 R5
ST 2629 10/91

DISCLAIMER

An integrating image detector for high energy neutrons.

Chris Morris, V. Armijo, L.G. Atencio, A. Bridge, A. Gavron, G. Hart, K. Morley,
T. Mottershead, G.J. Yates, and John Zumbro

Los Alamos National Laboratory
Los Alamos, NM 87544, USA.

ABSTRACT

We describe an integrating cathode-pad read-out wire chamber for imaging high energy neutrons. This technology allows construction of a detector with a wide dynamic range (10^4), which is gatable, easily read out, and provides millimeter scale resolution. Results from a prototype 48 × 48 pixel array are presented.

1 INTRODUCTION

In this paper we describe the motivation behind the high energy neutron radiography work in Los Alamos, and describe and present some results from an integrating, imaging detector for high energy (30-600 MeV) neutrons.

Radiography provides a method of non-destructive evaluation of objects with internal structure. Quantitatively, lengths, l_i, through an object can be extracted by measuring the attenuation of a penetrating beam of neutral particles such as neutrons or X-rays:

$$N = N_0 e^{-\Sigma \frac{l_i(x,y)}{\lambda_i}}, \quad \lambda_i = \frac{1}{\rho_i \sigma_i}. \tag{1}$$

Where $N_0(x,y)$ is the incident flux, $N(x,y)$ is the transmitted flux, λ_i are mean free paths, and $l_i(x,y)$ are a set of lengths of materials in the object being radiographed. Ideally, if contributions from detectors and other sources of error are ignored, the precision of the measurement can be evaluated in terms of the Poisson statistics associated with the transmitted flux. For a single component material Eqn.. 1 reduces to:

$$l(x,y) = \lambda \ln\left(\frac{N(x,y)}{N_0(x,y)}\right). \tag{2}$$

and the error in l is given by:

$$\Delta l(x,y) = \frac{dl}{dN}\Delta N(x,y),$$
$$\Delta l(x,y) = \frac{\Delta N(x,y)}{N(x,y)}\lambda = \sqrt{\frac{1}{N(x,y)}}\lambda. \tag{3}$$

Where we have applied the Gaussian approximation, appropriate for large numbers, to get the error in the transmitted flux, and we have ignored the fluctuations in the incident flux. An optimum λ for radiographing an object of a given thickness can be calculated by taking the derivative of $\Delta l(x,y)$ with respect to λ and setting it equal to zero. This gives:

$$e^{-\frac{l}{2\lambda}} - \frac{l}{2\lambda}e^{-\frac{l}{2\lambda}} = 0 \Rightarrow \lambda = \frac{l}{2}. \tag{4}$$

The advantage of neutrons for radiographing thick objects becomes immediately apparent when one compares the maximum mean free paths of photons with those of high energy neutrons in different media. This comparison is present in table 1) for a high-Z and a low Z material.

Table 1. Mean free paths for photons, λ_γ, and neutrons, λ_h.

Material	λ_γ (gm/cm^2)	λ_h (gm/cm^2)
Li	20	55
U	20	120

Another feature of high energy neutron radiography which is useful for our particular application is the smaller λ low Z materials than for high Z materials. This implies neutrons are especially useful for radiographing low Z material surrounded by a high Z material

High intensity sources of high energy neutrons are available using proton induced spallation. Good length to diameter ratios (L/D) are available from spallation targets. However, imaging detectors for high-energy neutrons have not been developed.

2 DETECTOR

Several issues drive the design of the detector. The interactions of high energy neutrons are predominately due to elastic or quasi-elastic collisions with nuclei. Many of these interactions produce energetic charge particles which can be detected using a variety of techniques. However, the ranges in most media are much longer than the two mm position resolution needed in our application. We avoid the position resolution broadening due to the range of the charged particles by using a thin converter followed by a thin position sensitive detector. For such a transmission detector the position resolution approximately given by $\Delta x = \tan(\theta)t$, where θ is the mean angle at which the charged particles are emitted, and t is the thickness of the converter plus detector. We have measured $\tan(\theta) = .4$ in a previous experiment where tracking chambers were used as the position sensitive neutron detector.[1] The detector efficiency, which is also proportional to t, and the position resolution are coupled. The best converter is one with the shortest interaction length. We have chosen tungsten. We have used an integrating cathode-pad read-out chamber for the detector. In this detector the positive charge created by avalanches near an anode plane is collected on a set of 48×48 conducting pads placed on 2.5 mm centers on a printed circuit board which forms the upstream cathode of the wire chamber. Photographs of the detector are shown in Figure 1.

The charge deposited on each of the pads in the detector was stored on a 220 pf capacitor, until it was readout through a multiplexer, an amplifier and into a CAMAC ADC. Leakage currents limited the readout time to be less than about 10 seconds in order to avoid loosing too much of the signal. The multiplexing was arranged so that each of the 48 columns of the detector was multiplexed into a common ADC. In total 48 ADC channels were used, one for each row.

Tests of the performance of this technique were made using a single element detector with a prototype of the electronics. Some results obtained with an ^{55}Fe X-ray source for the integrated charge as a function of counting rate are shown in Figure 2. The width of the distribution of the induced charge is compared with the result expected from the Poison distribution expected from counting statistics. Over the measured range there appears to be no significant departure from the result expected from a perfect detector, i.e., the detector is quantum statistics limited.

There is an additional term in the expected width when detecting particles for which there are fluctuations in the deposited charge such as neutrons. The can be expressed by relating the effective efficiency (*DQE*), measured by the fluctuation level, to the actual efficiency of the detector (EFF) for registering an incident particle. For particles which induce a mean charge q, with a fluctuation of σ.

$$DQE = \frac{EFF}{\left(1+\left(\frac{\sigma}{q}\right)^2\right)} \qquad (5)$$

We have measured $\sigma/q=1.67$ for the charge distribution in a wire chamber induced by high energy interactions in a previous experiment.[1] With a 1.5 mm tungsten converter we expectedEFF=1.3%, and DQE=0.4%

3 RESULTS

We have used the detector in the 30° R beam line at the WNR facility at Los Alamos Neutron Scattering Center (LANSCE) to image a test object. The details of the test object are shown in Figure 3. Data were taken at a set 9 angles between 0 and 180 degrees. The object was located about 20 m from the spallation source giving a flux of about 7×10^5/cm^2/sec. A two hour run was sufficient to obtain 0.1% statistical precession in a 2.5×2.5 mm^2 pixel at this flux. The transmitted flux was about 1/5 of the incident flux at the center of the object. This gives a detector quantum efficiency (DQE) of about 3×10^3 in reasonable agreement with our expectations.

The actual errors in our measurement of the transmitted flux had contributions from temperature induced fluctuations in the electronic gain, and beam intensity-dependent fluctuations in the chamber gain due to build up of charge on the areas of the cathode circuit board. The residual effects after our best efforts to correct for these systematic effects limited the precision of our measurements to about 0.4%. Never the less we have been able to achieve a sensitivity sufficient to clearly observe the effect of the 12.7 mm and the 6.3 mm diameter holes in the polyethylene insert in the test object in single views. This is shown in Figure 4. In addition a clear signal of the 3.2 mm diameter hole was obtained in the tomographic reconstruction of the data, suing a filtered back projection algorithm as can be seen in Figure 5. In to filtered back projection the object has been reconstructed using a maximum entropy tomographic algorithm. This produced fewer artifacts than the filtered back projection. The results are displayed in Figure 6.

4 CONCLUSIONS

We have described the construction of an integrating imaging detector for high energy neutrons. We were able to obtain a DQE of about .4 %. We demonstrated a sensitivity to structure in a test object at the 0.6% level in transmitted flux, looking through up to 160 gm/cm^2 of uranium using a white source of spallation neutrons. We will continue our work in the next running period with a larger detector build on 1.8 mm centers. The new circuit boards will have more copper coverage to avoid the problem with charge build up, and will rotate the test object more frequently so that we average over gain instabilities. In addition we are building a new spallation target, with it's axis aligned on the beam line, in order to increase the L/D ratio.

5 REFERENCES

[1] A. Gavron, *et al.*, contribution to this conference

[2] C. L. Morris, L. G. Atencio, G. C. Idzorek, and S. L. Morris, "Two-Dimensional, Beam-Image Monitor,"*Nucl. Instrum. Methods A* **269**, 333 (1987).

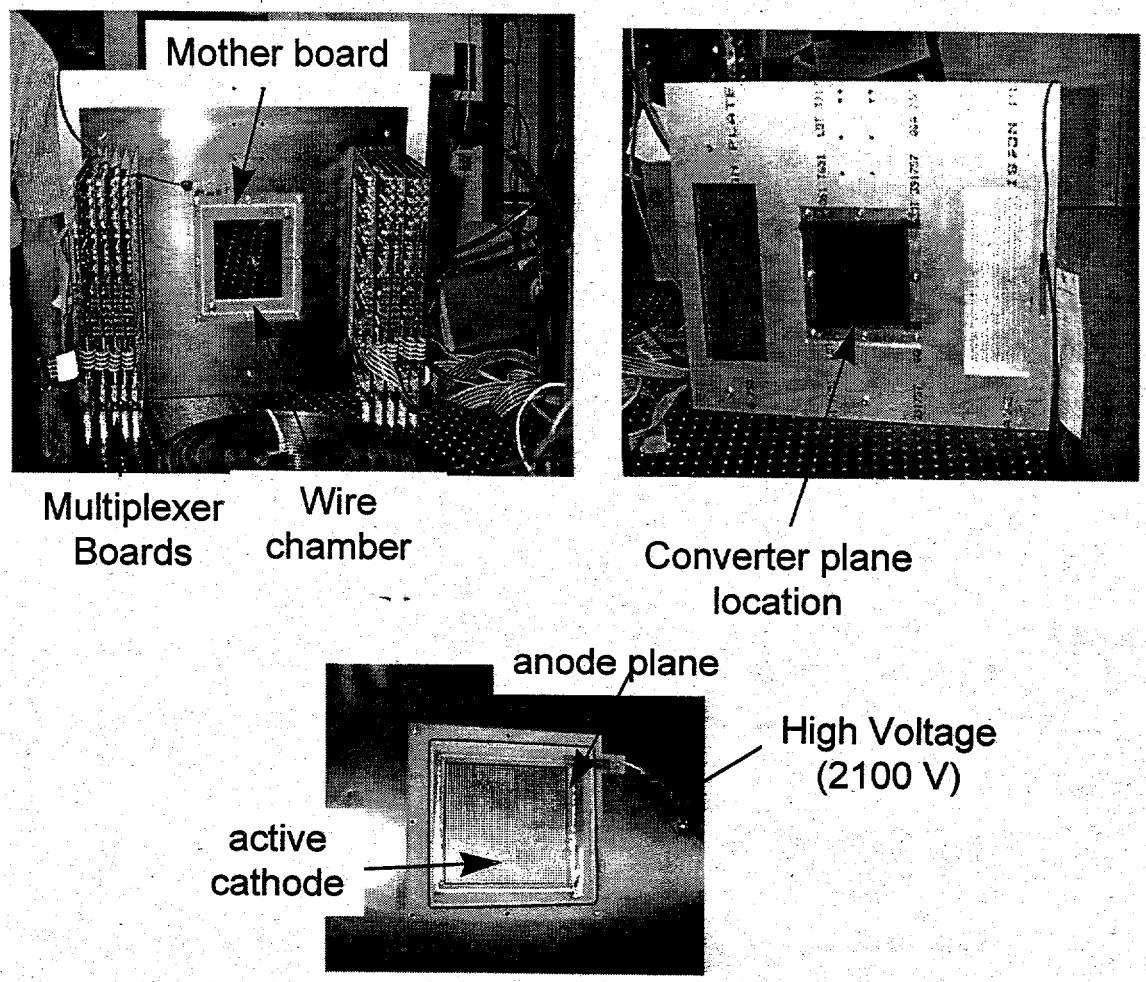

Figure 1: Photographs of the detector.

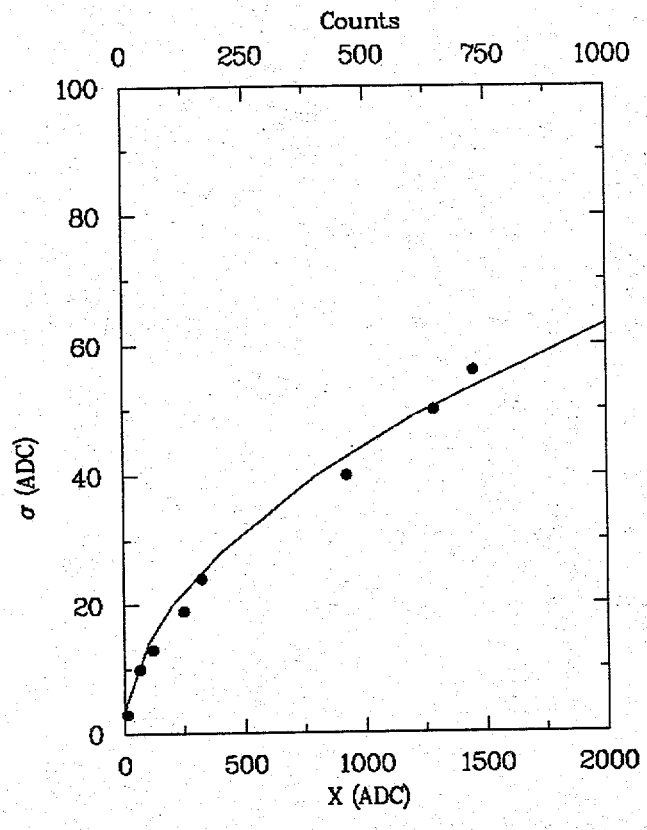

Figure 2: The width of the induced charge distribution (in ADC channels) as a function of number of detected counts (top axis). The measurements were made using an ^{55}Fe 6 keV X-ray source. The solid points are the standard deviation [σ (ADC)] of an ADC distribution, which is plotted as a function of the peak ADC channel [X (ADC)]. The solid line shows the standard deviation expected from counting statistics (the quantum limit).

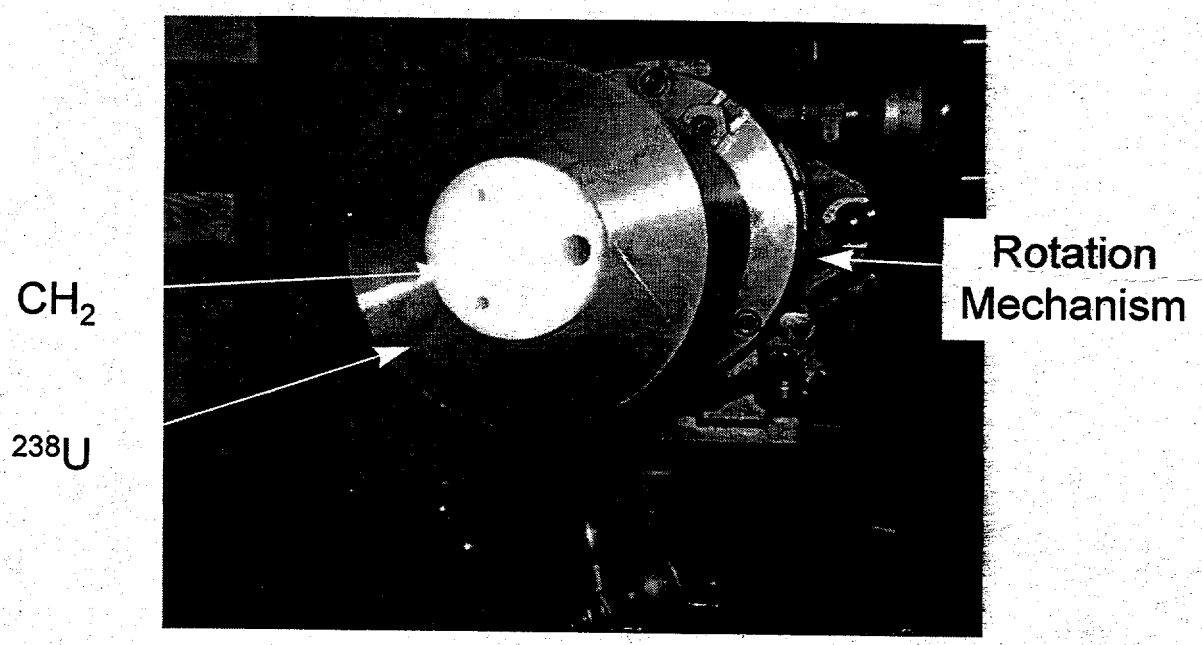

Figure 3: A picture of the test object. The outer cylinder was ^{238}U with an outer diameter of 15.24 cm, and an inner diameter of 7.24 cm. The center cylinder was fabricated from polyethylene. Three holes with diameters of 12.7, 6.3 and 3.2 mm were drilled through the cylinder. The beam direction was normal to the axis of the cylinder.

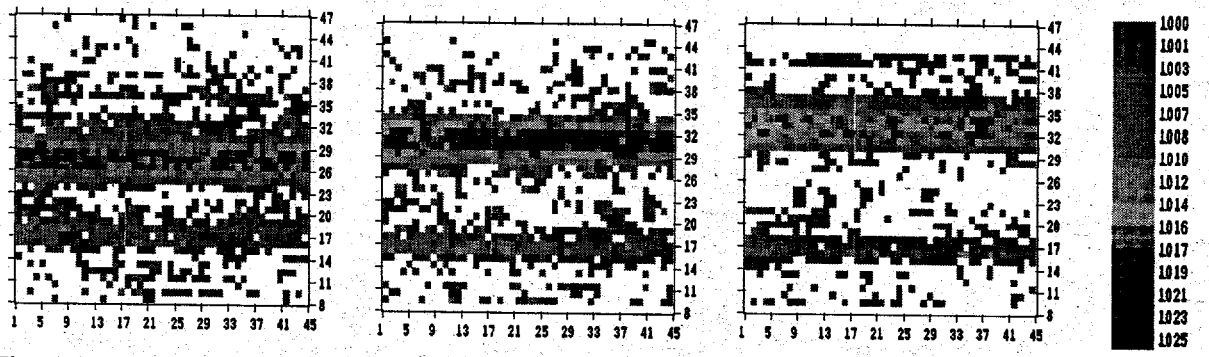

Figure 4: Histograms of the ratio of the images made with a polyethylene insert with holes to one without holes. The Z scale, displayed at the right, is 1000 time the ratio. The horizontal and vertical axis are pixel number in 2.54 mm steps.

a.)

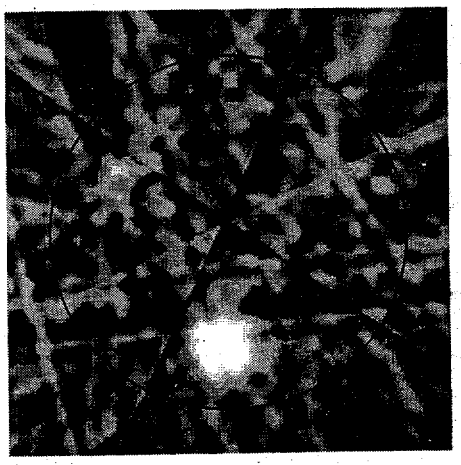

b.)

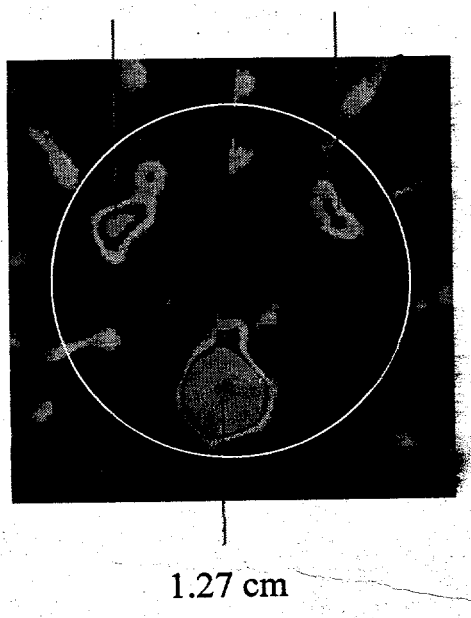

Figure 5: Results of a filtered back projection reconstruction made using 9 images (every 20°) a)unfiltered, b)filtered to remove some of the artifacts.

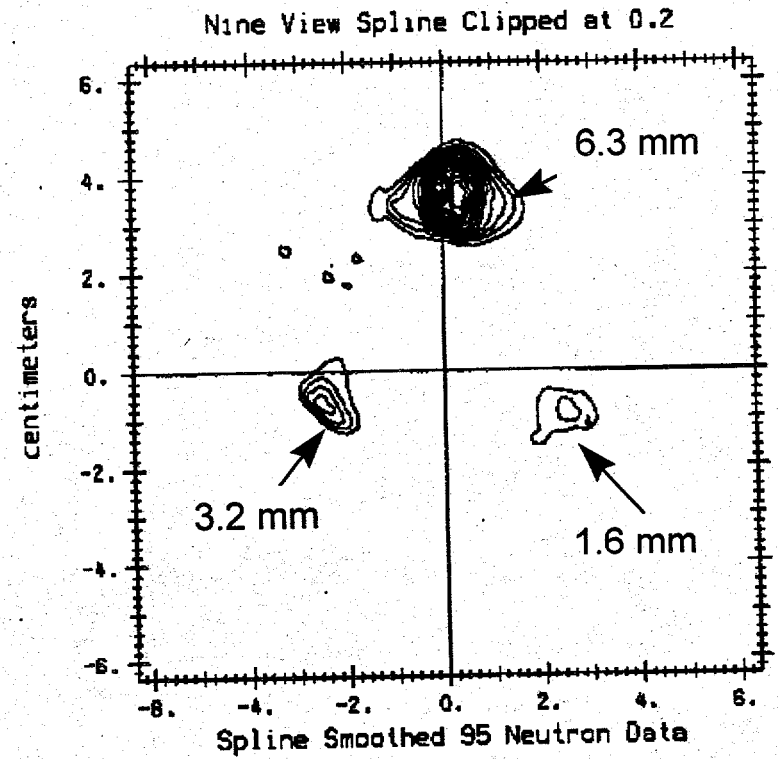

Figure 6: Results of maximum entropy reconstruction of the object using the same 9 images as in Figure 5.